AIMS Biophysics, 4(1): 107-120.
DOI: 10.3934/biophy.2017.1.107
Received: 07 November 2016
Accepted: 24 January 2017
Published: 06 February 2017

http://www.aimspress.com/journal/biophysics

Research article

Membrane-induced interactions between curvature-generating protein domains: the role of area perturbation

Nily Dan *

Department of Chemical and Biological Engineering, Drexel University, 3101 Chestnut St, Philadelphia PA 19104, USA

*** Correspondence:** Email: dan@coe.drexel.edu; Tel: +1-215-895-6624; Fax: +1-215-895-5837.

Abstract: Membrane deformation by asymmetric crescent-shaped proteins such as BAR-domains is calculated, using a mean field model that accounts for both bending and area stretch deformations. The penalties associated with membrane bending and area perturbation lead to moderately long-ranged (order 10 nm), non-monotonic, membrane-induced interactions between proteins that may prevent the formation of closely packed aggregates. As a result, BAR-domain proteins may favor the formation of an ordered array with a specific separation between domains whose spacing is set by the ratio between the bending and area stretch moduli.

Keywords: BAR domain; Amphiphysin; membrane perturbation; Helfrich model

1. Introduction

BAR (Bin-Amphiphysin-Rvs167) domain proteins are key players in cellular membrane remodeling, participating in processes such as endocytosis, trafficking, division, or migration and ubiquitous in species from insects to human [1–6]. BAR-domains are dimerized through a helical coiled-coil motif to form elongated, positively-charged crescent structures (see, for example, [7]). Electrostatic interactions between the dimer and negatively charged phospholipids such as phosphatidylinositol (4,5)-bisphosphate ($PI(4,5)P_2$) localize the protein at the membrane interface, where the protein's crescent shape causes a corresponding deformation in the bilayer. Additional curvature may be induced through the insertion of amphipathic helix "wedges" that disrupt the structure of the outer leaflet [3,4,8,9,10]. BAR-domains or proteins induce the formation of highly

curved regions such as tubules [11,12], where the formation of ordered linear arrays of the proteins on the membrane surface leads to large-scale remodeling [13,14].

The bending induced by the adhesion of BAR-dimers deforms the preferred flat geometry of the membrane, leading to an energetic penalty. Theoretical models of bilayer/BAR-domain assemblies find that this bending penalty depends on the properties and orientation of the interacting domains [15,16]; Protein aggregation minimizes the area of perturbed membrane and thus is favoured. The models predict that the interactions between proteins oriented normal to the surface (and parallel to each other) are purely repulsive, so that their aggregation minimizes the area of perturbed membrane, while the interactions between proteins parallel to the bilayer surface are purely attractive [15,16]. The result in either limit is overall membrane curvature as displayed by tubular geometry [15,16]. It is interesting to note that local segregation of lipid species in mixed bilayers, triggered by domain adsorption, has only a minor effect on the overall membrane curvature [17–21], suggesting that analysis based on the assumption of one-component lipid bilayers is still applicable to mixed systems.

Previous models of bilayer perturbation by BAR-domains account for bending deformation only. However, lipid assemblies change their area under pressure or local deformation [22], with an effective *area stretch modulus* that is comparable in magnitude to the bending modulus: For example, in phosphatidylcholine (PC) membranes the bending modulus is of order 10^{-19} J, while the area stretch modulus is of order 0.2 N/m (e.g. [23], which-translated to energy units (using a characteristic area per lipid of 70Å^2 [24,25]) is ~1.5 10^{-19} J. Indeed, recent simulations have shown, that the interactions between BAR-domains strongly depend on membrane tension [26,27]. Previous models of protein-induced membrane perturbation show that (even in tensionless bilayers) the perturbation of local bilayer structure due to the presence of proteins depends on both the bending and area stretch moduli [28,29]. Yet, as noted, to date theoretical models of membrane-mediated interactions between BAR-domains consider only membrane curvature, neglecting the potential effect of the area changes [15,16,18].

This paper explores the role of the area stretch modulus on membrane-induced interactions between crescent-shaped, asymmetric proteins such as the BAR-domains. The model takes into account that the binding between the domain and the bilayer causes two types of deformations: A curvature one (since the bilayer "molds" to fit the more rigid protein structure), and a packing one that arises from (i) perturbed density of the lipids bound to the domain (e.g. because of electrostatic interactions, insertion of amphipathic helices, etc.), and (ii) the coupling between local curvature and lipid packing arising from the associated splay. The inclusion of the area stretch modulus has an effect that is not only quantitative, but also qualitative, on membrane-induced interactions between proteins [28,29]. In particular, accounting for the bending stiffness alone leads to purely attractive interactions. However, the protein-induced local area perturbation (and a non-zero area modulus) yields a *non-monotonic* interaction profile between domains that can give rise to ordered arrays with a preferred spacing-even in the absence of direct protein-protein interactions [28,29]. The model used is a mean field, self-consistent one based on the Helfrich approach [30] that calculates the optimal membrane perturbation profile resulting from an induced deformation by free energy minimization. To evaluate the role (if any) or area perturbations, the analysis focuses on tensionless membranes: First, the self-assembled nature of lipid membranes and their (low, but finite) permeability to water means that imposed tension can be relaxed after a period of time, so that an equilibrium analysis such a the one discussed here is more appropriate for tensionless systems. Second, imposed tension

emphasizes the role of area perturbation when compared to curvature penalties; The analysis of the tensionless membrane will provide the lower limit for the effect of the area perturbation, and enable a clear comparison to curvature effects.

2. Materials and Methods

2.1. Mean field model

The Helfrich mean-field model is used to calculate the free energy of a membrane as an expansion in the local curvatures [30]

$$F = \int_A \left\{ B + \frac{K}{2l_0^2}\left(C_1 + C_2 - C_0\right)^2 + \frac{\bar{K}}{l_0^2} C_1 C_2 \right\} dA \tag{1}$$

here F is the free energy (in units of kT, where k is the Boltzmann constant and T the temperature). The membrane free energy is written in terms of the bilayer moduli: B is the compressibility modulus that accounts for the interfacial tension and molecular packing, K the bending rigidity, $\bar{K}$ the Gaussian modulus, l_0 the thickness of the interfacial layer, and C_0 is the spontaneous curvature (preferred curvature) of the bilayer, which is typically zero for bilayers. The energy penalty for deformation depends on the deformation profile—C_1 and C_2 are the principle curvatures (all curvatures are dimensionless, given by the ratio between the bilayer thickness and the relevant radius of curvature). It should be noted that, although eqn (1) is an expansion to 2nd order in curvature, it has been shown to apply even to highly curved surfaces [31,32].

Binding between proteins and the bilayer imposes a perturbation in both the local curvature and the packing density (due, for example, to electrostatic screening of lipid-lipid interactions by the oppositely charged protein ones). Since the membrane is self-assembled, the lipid packing density (defined by the area per lipid, or, inversely, by the surface density) is linked to the local thickness of the membrane by an equation of state. The simplest relationship is that of tail volume conservation, namely, that the area per lipid times the local thickness is equal to the tail volume. More sophisticated ones account for such contributions as water penetration into the membrane core [33]. In all cases, however, the local thickness of the membrane can be coupled to the area per lipid so that the area perturbation caused by protein incorporation can be accounted for by considering the thickness of the membrane, or the dimensionless thickness perturbation $\Delta(\bar{r}) = (l(\bar{r}) - l_0)/l_0$, where l_0 is the unperturbed thickness of the layer, and $\bar{r}$ the distance from some fixed point.

Defining the local perturbation through the membrane thickness profile allows coupling it to the local curvature: In caretsian coordinates with z axis long the bilayer thickness and (x,y) in the membrane plane (see Figure 1), $C_1 = C_{i1} + l_0^2 \partial^2\Delta/\partial x^2$ and $C_2 = C_{i2} + l_0^2 \partial^2\Delta/\partial y^2$, where C_{i1} and C_{i2} are the *initial* curvatures of the bilayer before deformation (for a detailed derivation see Supplemental Materials).

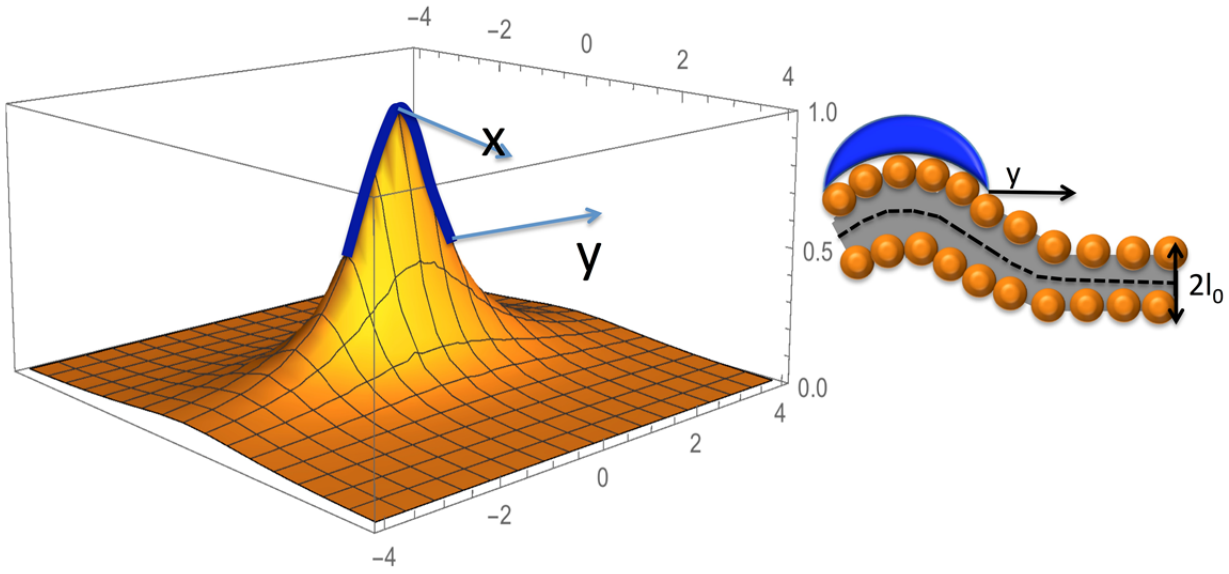

Figure 1. Membrane perturbation by an adsorbed crescent protein, such as the BAR-domain dimer. The blue curve represents a model crescent protein. The y coordinate describes the distance in the direction along the backbone of the crescent, while the x coordinate denotes the transverse distance: (0.0) defines the center of the protein. The z coordinate describes the local perturbation to the membrane's outer surface, and relates to Δ, the thickness perturbation. Note that the z scale is exaggerated to emphasize the deformation. The curvature of the protein is exaggerated here for illustration purposes. The side sketch shows an enlargement of the membrane/protein interface. *Figure drawn using Mathematica* ©

In the case of crescent proteins such as the BAR domains, their shape induces a local *cylindrical* curvature in the membrane so that $C_2 = 0$. If the membrane has zero spontaneous curvature and is initially flat (on a local basis) so that $C_{i1} = C_{i2} = 0$, free energy minimization yields the Euler-Lagrange equation [34]

$$B\Delta + \frac{K}{2} l_0^2 \nabla^4 \Delta = 0 \tag{2}$$

The solution of this equation is of the form

$$\Delta(\bar{r}) = \sum_{n=0}^{3} a_n \exp\left[(-1)^{\frac{(2n+1)}{4}} \frac{\bar{r}}{\lambda} \right] \tag{3.a}$$

where $\lambda = (2Kl_0^2/B)^{1/4}$ and $\bar{r}$ is the 2D planar distance from the protein boundary (namely $\sqrt{(x^2 + y^2)}$ in Cartesian coordinates such as shown in Figure 1). An alternate representation of the profile is

$$\Delta(\bar{r}) = \left(b_1 e^{\bar{r}/\lambda} + b_2 e^{-\bar{r}/\lambda} \right) \left(b_3 \sin\left[\bar{r}/\lambda \right] + b_4 \cos\left[\bar{r}/\lambda \right] \right) \tag{3.b}$$

The decay profile depends on the geometry of the system and the boundary conditions at the interface between the protein and the membrane (see Figure 1). The length to width ratio of BAR-domains is relatively high (ranging from 7 to 14, depending on the type of domain [35]). As a result the membrane perturbation can be decoupled into an "edge" orientation, in the direction parallel to the domain axis (y in Figure 1), and a "center" one, extending in the direction perpendicular to the domain axis (x in Figure 1).

The boundary conditions are therefore different for x and y: In the "edge" orientation the curvature at the domain boundary is set by that of the dimer, C_D, and the thickness perturbation is given by some value, Δ_0. In the center orientation there is no imposed curvature and the only boundary condition at the protein interface is that of Δ_0. In addition, at the midpoint between adjacent proteins the 1st and 3rd derivatives of the Δ are zero. It should be noted that the values of these boundary conditions will differ between the top monolayer- which is in direct contact with the protein, and the bottom monolayer, which is not (Figure 1). The analysis here focuses on the top leaflet whose deformation and energetic penalty are likely to dominate the system and can be directly linked to the protein properties. The bottom monolayer's contribution can be calculated in a similar manner, but the applied boundary conditions are not as directly correlated to the protein characteristics, and therefore harder to define.

Once the thickness perturbation profile is determined, it can be substituted into eqn (1) and integrated as a function distance from the protein boundary:

$$F_x(h) = L\int_0^h \left\{ B\Delta^2 + \frac{1}{2}K\frac{d^2\Delta}{dx^2} \right\} dx \tag{4.a}$$

or

$$F_y(h) = W\int_0^h \left\{ B\Delta^2 + \frac{1}{2}K\frac{d^2\Delta}{dy^2} \right\} dy \tag{4.b}$$

where 2 h is the separation between adjacent proteins, L is the contour length of the protein, and W the width.

3. Results

The length to width ratio of BAR-domains is relatively so that the membrane perturbation can be decoupled into two orientations: "Edge" in the direction parallel to the domain axis (y in Figure 1), and "center" in the direction perpendicular to the domain axis (x in Figure 1). In both directions, the adsorbed domain causes a local perturbation in the lipid packing density at the domain/bilayer contact that is defined by a value Δ_0 determined by the domain-membrane interactions. However, in the end orientation the domain also imposes a local curvature that is set by the structure of the specific protein. Substituting these boundary conditions into eqn 3 yields for an isolated protein where h, the distance between adjacent proteins, is taken to be infinite:

$$\Delta(x) = \Delta_0 e^{-x/\lambda} \cos\left(\frac{x}{\lambda}\right) \tag{5.a}$$

and

$$\Delta(y) = e^{-y/\lambda}\left\{\Delta_0 \cos\left(\frac{y}{\lambda}\right) + C_D \frac{\lambda^2}{2l_0^2} \sin\left(\frac{y}{\lambda}\right)\right\} \tag{5.b}$$

$\lambda = (2Kl_0^2/B)^{1/4}$ is the characteristic membrane perturbation length. High values of λ indicate a large resistance to bending, which leads to a perturbation profile that is relatively low in curvature but extends further from the protein boundary, thereby incurring a higher area perturbation penalty. A small value of λ corresponds to a significant resistance to area perturbation, so that the profile decays rapidly with distance from the protein boundary, at a cost of locally high curvatures.

Figure 2 shows the optimal membrane perturbation profile imposed by a BAR domain as a function of the dimensionless distance from the center (2.A) and the edge (2.B). The values chosen for Δ_0 and the protein curvature, C_D are representative of BAR-domain proteins: Δ_0 depends on parameters such as the charge density of the membrane and the protein and the solution ionic strength, as well as the additional effect of the wedge helices inserted in the bilayer, so that $\Delta_0 = 0.1$ is a reasonable estimate [36,37]. Note that the center profile scales linearly with Δ_0 (eqn 5.a) so that it defines the scale of the perturbation. C_D, the domain curvature, is given by l_0/R_D, where R_D is the radius of curvature of the BAR-domain dimer, and can range from ~0.07 to ~0.3 for the F and N-BARs, or order –0.05 for I-BAR proteins [35]. A more detailed explanation of the values chosen here is in the "Discussion" section.

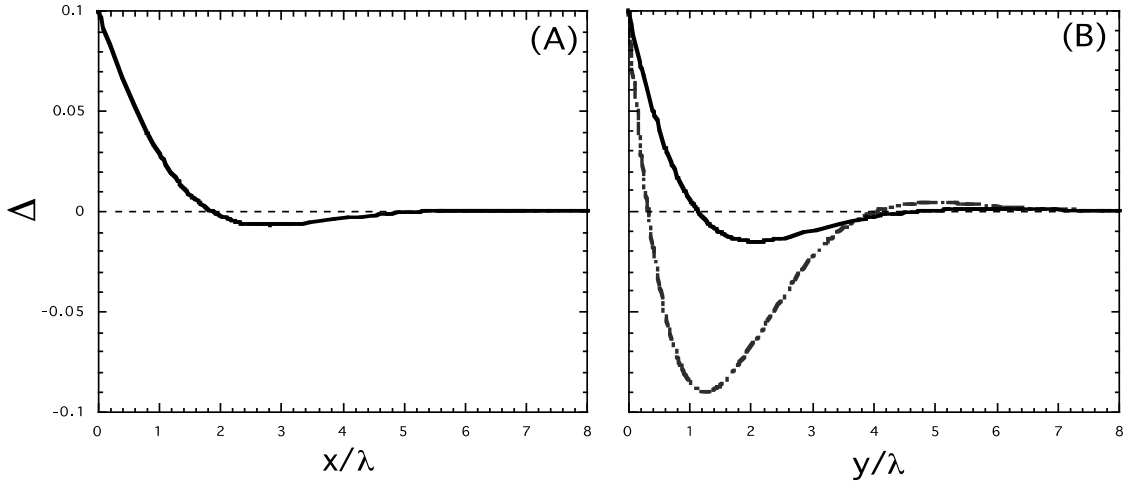

Figure 2. Dimensionless bilayer thickness perturbation as a function of the dimensionless distance from a single (isolated) crescent protein (based on eqn 5). (A) Center perturbation, (B) end perturbation. The protein- imposed thickness deformation is taken to be relatively weak: $\Delta_0 = 0.1$, i.e. 10% of the membrane thickness. The protein dimensionless curvature, namely, bilayer (equilibrium) thickness divided by the protein radius of curvature, is equal to 0.1 (solid line) and 0.5 (dashed line).

The free energy penalty due to membrane perturbation by a single (isolated) BAR domain can be calculated, self-consistently, from the perturbation profile by integrating over the optimal profile Δ (eqn 4, when h- > ∞). As in the profile calculation, the penalties due to the edge and the center deformations are decoupled, so that the total energy penalty per isolated BAR-domain (in units of kT) is given by

$$F_{tot,\infty} = \left(\frac{K}{8Bl_0^2}\right)^{1/4} \left\{ \left(L+W\right) B\Delta_0^2 + KC_D^2 \frac{W}{2l_0} \right\} \tag{6}$$

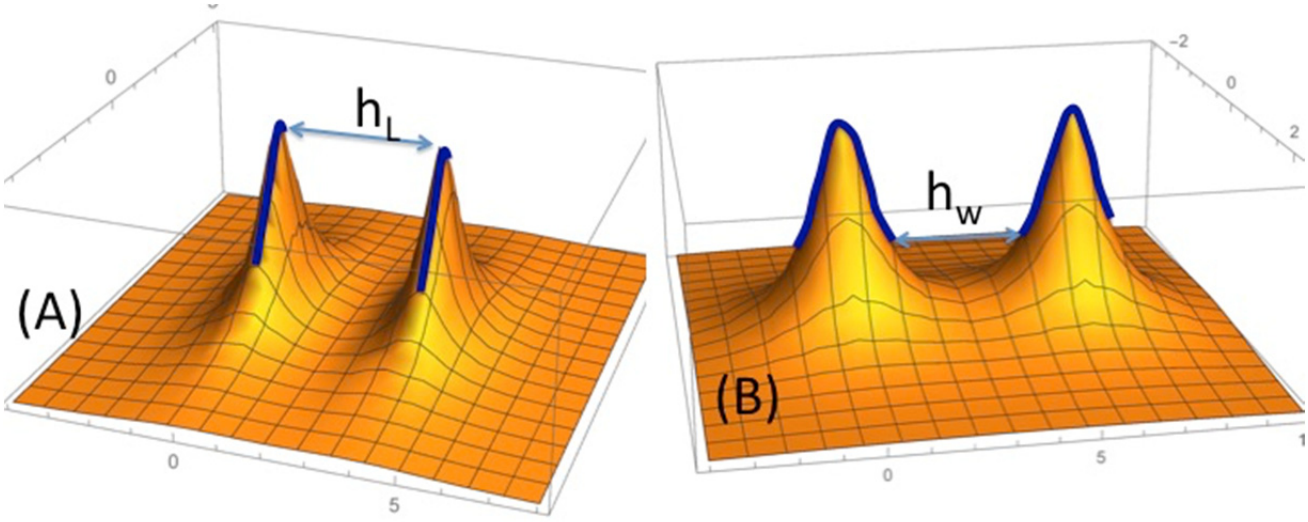

Figure 3. Interactions between crescent-shaped proteins depend on their relative orientation. The blue curves represents the location of the model crescent proteins. (A) center to center, and (B) end to end. h_L defines the spacing between the protein edges in the center-to-center, and h_W between their ends in the end-to-end. *Figure drawn using Mathematica* ©

When two domains approach each other, their membrane-induced perturbation profiles overlap, modifying the perturbation profiles and the associated energetic penalty. As in the single-domain case, the overlapping profile depends on the relative orientation: end-to-end or center-to-center, as sketched in Figure 3 (it should be noted that other approach angles are clearly possible, but it has been shown that these two orientations dominate [26]). The resulting perturbation profiles, for several end-to-end separation values, are plotted in Figure 4. At large spacings, the perturbation profiles do not interact. As the distance decreases, the deformation profiles start to overlap, leading to a change in the optimal membrane thickness profile.

The energetic end-to end penalty due to the adsorption of a single protein in a dense array is plotted in Figure 5 as a function of the distance between proteins. As suggested by the perturbation profiles (Figure 3), proteins start to interact when the distance between them is of order 8λ (recall that h is *half* the separation between adjacent proteins). The inset shows a magnification of the shallow attractive minimum at a distance of order h = 3λ. At closer distances, the large deformation due to the overlapping perturbation profiles causes a significant energy barrier. At contact (h = 0) there is no energetic penalty since there is no membrane between the proteins.

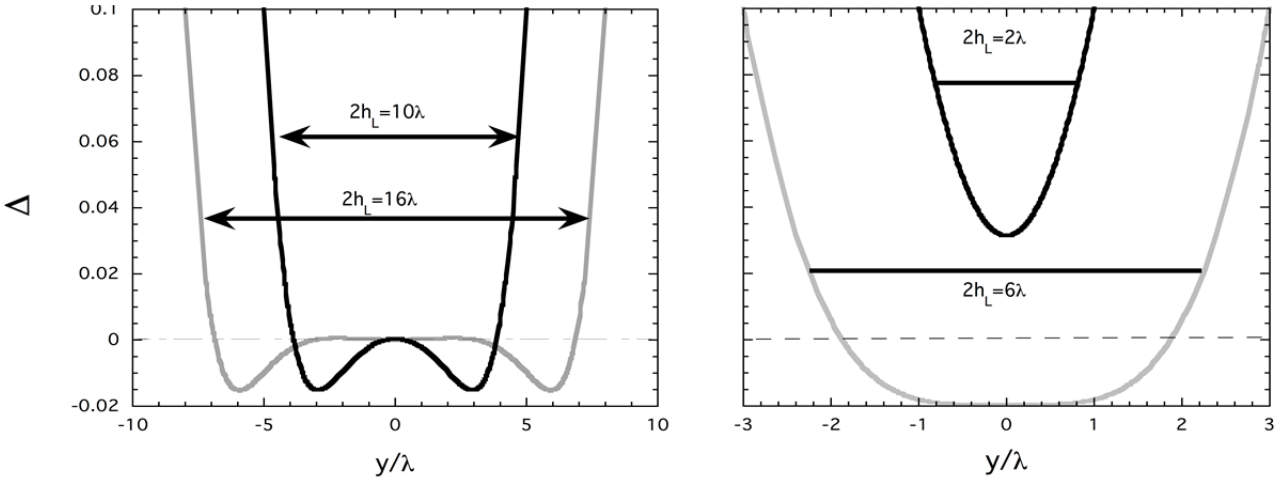

Figure 4. The membrane perturbation profile as a function of distance from two interacting crescent proteins in end-to-end orientation. The dimensionless curvature is 0.1, and the thickness perturbation is $\Delta_0 = 0.1$. The overall separation between the protein ends is given by $2h_L$.

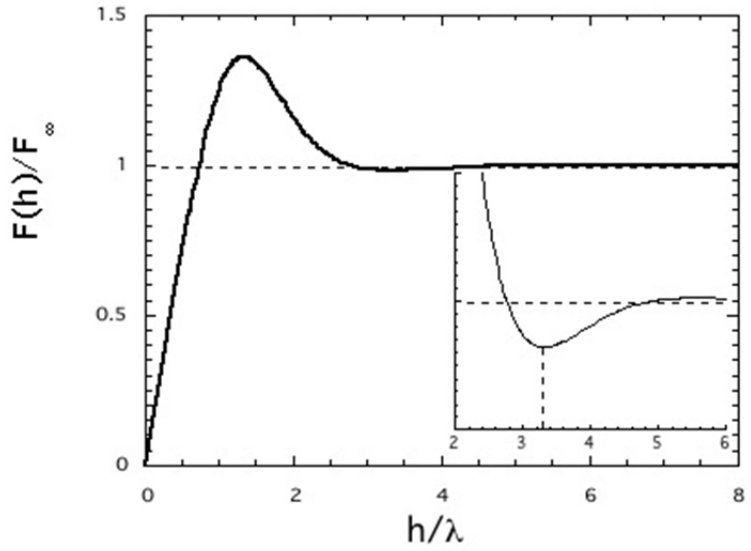

Figure 5. The membrane free energy penalty for an end-to end- perturbation due to a single adsorbed BAR-domain, as a function of the dimensionless distance between adjacent domains, h. $F(h)/F_\infty$ is the free energy relative to the isolated domain case. The dimensionless curvature is 0.1, and the thickness perturbation is $\Delta_0 = 0.1$.

4. Discussion

Lipid membranes are self-assembled structures whose surface area is set by the preferred packing density of the constituent lipids. The preferred packing density is sensitive to such parameters as the solution ionic strength or pH (see, for example, [38,39]), or can be modified by

imposing membrane curvature [40]. The adsorption of proteins on the membrane surface can perturb the lipid packing on a local scale (e.g. by screening electrostatic interactions), giving rise to a perturbation profile and an associated energy penalty. The membrane response to this perturbation is defined by a characteristic length scale (eqn 3), $\lambda = (2Kl_0^2/B)^{1/4}$, where K is the bending modulus, B the area stretch modulus, and l_0 the bilayer thickness.

λ, the membrane perturbation length, is independent of the type or magnitude of the imposed local perturbation, a function of the bilayer properties only. In systems where the bending modulus is large relatively to the area modulus, λ is large and perturbations decay slowly, with a bilayer thickness profile that minimizes local curvature. In systems where $B >> Kl_0^2$ the perturbation profile decays rapidly so as to minimize the area of perturbed lipid packing, at a cost of high curvature. (Assuming that the membrane area is fixed corresponds to a value of B = 0, where there is no "natural" membrane deformation length-scale. In such cases, the area affected by the perturbation is set by the inclusion/protein size—see, for example, [15,16]).

The adsorption of crescent-shaped inclusions, such as BAR-domain proteins, on a lipid membrane causes both a bending and a packing deformation at the membrane/protein boundary. Due to their highly aniosotropic shape (length >> width), the perturbation profiles imposed by BAR-domain proteins can be decoupled into two orientations (Figure 1): Perpendicular to the protein length, where the perturbation is dominated by packing, or thickness deformation, and parallel to the protein length, where the perturbation combines both packing deformation and an imposed curvature.

The magnitude of the imposed thickness perturbation (which is proportional to the lipid packing perturbation), Δ_0, depends on parameters such as the charge density of the protein, the charge density of the lipid bilayer, and the solution ionic strength. In the case of BAR-domains, additional packing perturbation may be caused by the protein's helical "wedges"[3,4,8,9,10]. Therefore, the value of Δ_0 can vary widely between different BAR-domain/bilayer systems and as a function of solution conditions.

Unlike other types of proteins (e.g. transmembrane proteins), BAR-domains also impose a curvature on the membrane. The nominal curvature of BAR-domain proteins can be estimated through the ratio between the membrane thickness and R_D, the radius of curvature of the BAR-domain dimer, i.e. $C_D = l_0/R_D$. This value ranges from ~0.07 for F-BAR to ~0.2 for N-BARs (the curvature of I-BARs is inverse, with $C_D \approx -0.05$) [35], although it can vary greatly depending not only on the protein curvature but also on the membrane thickness. For example, Amphiphysin has a radius that is approximately 11 nm, so that the imposed C_D on phosphatidylcholine (PC) membranes whose thickness $l_0$is can vary from ~3.5 nm to 4.4 nm [23,41]) can vary from 2.5–3.2. Furthermore, the insertion of "wedges" by the protein into the bilayer may also increase the imposed curvature beyond that of the protein dimer itself, depending on the number and nature of the amphipathic helix units and the properties of the bilayer.

Calculating the membrane perturbation profile that minimized the energetic penalty due to the inclusion of an isolated BAR-domain protein (eqn 5) yields an oscillating exponential decay whose characteristic lengthscale is λ and whose magnitude scales with the imposed perturbation values, Δ_0 and C_D. Figure 2 shows the membrane perturbation profile in the two principle directions for a thickness (or packing density) perturbation at the protein boundary of 0.1, or 10%, with two values of the imposed curvature: $C_D = 0.1$, a value that is similar to that of the F-BARs or some N-BARs, and a high value of $C_D = 0.5$ to examine the effect of a potential upper limit. Note that intermediate

values of C_D will follow a perturbation profile that falls between these two values, while ones for C_D values lower than 0.1 will fall between this one and the $C_D = 0$ profile shown in Figure 2A.

As may be expected, the magnitude of the edge (parallel) perturbation that accounts for *both* packing and curvature deformations, is larger than that of the center perpendicular one. It is interesting to note that, despite the fact that the characteristic lengthscale is the same (= λ), the maxima and minima of the larger imposed curvature are located more closely to the protein boundary (see Figure 2B) that those of the weaker perturbation. Thus, more highly curved domains such as N-BARs may induce more pronounced perturbation than the weakly curved F-BARs, but the range of the imposed perturbation may extend to shorter distances from the protein boundary.

The oscillating perturbation profile differs from the one expected when considering only bending penalties, where the deformation is found to decay as a simple exponential from the protein boundary [15,16]. It is in agreement with the simulations of Simunovic, et al [13,14] who find clearly decaying oscillations in the Gaussian curvature of the bilayer and the lateral pressure per lipid (which is related to the packing density and, therefore the thickness) as a function of distance from the boundary of the BAR domain.

The perturbation penalty due to an isolated protein, F_∞ (eqn 6) describes the resistance of the bilayer to the adsorption of a single, isolated protein. Unlike the electrostatic interactions that drive the adsorption, which are highly sensitive to solution conditions such as ionic strength, the perturbation penalty is dominated by the membrane moduli and the magnitude of the induced curvature perturbation: As the moduli (K,B) increase, so does the energetic penalty. Due to the coupling between local bilayer thickness (or density) and curvature, the modification of one leads to a perturbation in the other (see, for example, [28,29])**.** As a result, even if there is no protein-imposed curvature (i.e. $C_D = 0$) the perturbation energy still depends on K, the bending modulus, and if there is no area perturbation ($\Delta_0 = 0$) the penalty still depends on the B, the area modulus. Thus, neglecting the contribution of area deformation (i.e. taking B = 0) may significantly underestimate the penalty associated with the domain-induced perturbation even if the perturbation is dominated by curvature, rather than area changes.

The value of the isolated protein energy penalty, F_∞ depends on the BAR-domain characteristics: C_D, Δ_0 and the length of the domain, as well as the bilayer moduli B and K. Rawicz, et al [23] find that for saturated lipids, membrane moduli for phosphatidylcholine (PC) membranes are in the range of $K = 10^{-19}$ J, B = 0.2 N/m and $l_0 = 3.5$ nm (these values vary with the tail length, and are consistent with other systems as well, e.g. [41]). As a concrete example, for Amphiphysin whose radius of curvature is approximately 11 nm, C_D is of order 0.3. The length of the protein is of order 20 nm [7]. As a result, F_∞ is of order 1 (i.e. the energy is equal to kT) for $\Delta_0 = 0$, i.e. when there is no thickness perturbation associated with the protein adsorption, and increases to order 10 when $\Delta_0 = 0.1$. For adsorption to take place, the protein adsorption energy must be high enough to compensate for this penalty, namely, in the range of 1–10 kT. If the energy released by the formation of an electrostatic bond (due to counterion release) is taken to be of order 1 kT, the adsorption energy of proteins like Amphiphysin should be of order 7–10 kT (see, for example, [42,43]). However, screening by water molecules at the bilayer surface has been shown to reduce the adsorption energy so that, for N-BAR domains, it may be on the order of ~3 kT [44]. These values are within the same order of magnitude as the membrane perturbation penalty, suggesting that the magnitude of thickness deformation that can be supported by the bilayer (i.e., if the deformation exceeds this value the protein will not adsorb)

must be low, unless other binding mechanisms (such as the insertion of the amphipathic helix wedges) bind the protein more firmly to the membrane and compensate for the higher deformation penalty [44].

Membranes can display spontaneous, thermally induced fluctuations whose magnitude depends on the type of constituent lipids and temperature: For example, the amplitude of thickness fluctuations in pure dimyristoylphosphatidylcholine (DMPC) or distearoylphosphatidylcholine (DSPC) is of order 0.4 nm over a broad range of temperatures, but that of mixed DMPC/DSPC systems range from ~0.35 nm at 35 °C to 1.2 nm at 65 °C [45]. The energetic penalty associated with such fluctuations is of order kT, and is therefore comparable in magnitude to the perturbation penalty associated with proteins with low imposed thickness (Δ_0) and curvature (C_D) values; The perturbation associated with BAR-domain proteins, and the resulting energetic penalty, may be an order of magnitude higher. However, it cannot exceed the ~5–10 kT range, when the membrane energetic penalty becomes higher than the adsorption energy gain.

Increasing the concentration of BAR-domain proteins in the membrane decreases the spacing between them. This leads to an overlap in the perturbation profiles of adjacent domains (see Figure 4) that modifies the profiles, and as a result the energetic penalty (Figure 5). When the spacing between proteins is relatively large ($h_L = 8\lambda$), the membrane recovers its equilibrium thickness in the center between the proteins and the associated energetic penalty is the same as that of the isolated domain. However, as the proteins approach each other the perturbation profile overlap; When the spacing is relatively close ($h_L \leq 6\lambda$), the membrane does not regain its preferred thickness. The deformation profiles induced by adjacent proteins in the center-to-center profiles show similar trends.

The effect of the separation between domains on the end-to-end energetic penalty is non-monotonic, as shown in Figure 5: While studies considering only the bending modulus (namely, implicitly taking B to be zero) find purely attractive interactions [15,16,18], accounting for the area stretch modulus introduces an energy barrier to aggregation at a spacing of order 2λ, preceded by a shallow minimum at $\sim 3\lambda$. The height of the barrier is roughly $F_B \approx 0.4F_\infty$, namely, approximately 5 kT. Thus, although the overall interaction between BAR-domains is attractive (since the perturbation penalty is minimized when h = 0), this barrier may prevent it from occurring. The probability of random protein motion overcoming the barrier so that aggregation takes place is proportional to $\exp(-F_B)$, namely, decreasing exponentially as the values of K and/or B increase. It should be noted that while Figure 5 focuses on the end-to-end arrays, the center-to-center interactions follow the same trend. The main difference between the two orientations is in the scale of the energetic penalty, since the end-to-end orientation accounts for both the area and bending deformations induced by the BAER-domain, while the center-to-center is due to only the area packing perturbation.

These results are in qualitative agreement with the molecular-scale coarse-grained simulations of Simunovic and Voth [26,27], who find that BAR-domains interact (when the membrane is tensionless) over distances of order 12 nm, an order of magnitude larger than the range expected for electrostatic interactions. This range is similar to the one predicted by the model presented here of $\sim 3\lambda$, which translates to a range of 6–10 nm for typical PC bilayers [23], and may be higher for stiffer ones. In addition, the simulations find that in the tensionless membrane, the energy gain due to protein aggregation is of order 6 kT [26,27]. This is comparable to the value of F_∞ in our model (which ranges between 1 and 10 kT depending on the magnitude of the thickness perturbation). This energy barrier may prevent, in certain cases, the formation of a closely packed cluster by the BAR-domains, yielding instead an ordered array with a spacing of order 3λ, namely, ~10 nm.

The distance between proteins, h, is inversely proportional to their concentration on the bilayer surface. As a result, the energy profile displayed in Figure 5 can be used to evaluate the phase behavior of adsorbed Bar-domains. At low concentrations (h large) the proteins do not interact and are expected to be distributed randomly on the surface. As the concentration increases, the proteins begin to interact. Due to the energy barrier at higher concentrations (smaller h values), it is likely that the proteins may order in an array whose spacing is associated with the shallow energy minimum at ~3λ (see Figure 5 inset).

5. Conclusion

A mean-field model is used to calculate the effect of the area stretch modulus on the properties of lipid bilayers perturbed by a crescent-shaped BAR domain. The results show that accounting for the area modulus gives rise to a non-monotonic perturbation profile, associated with non-monotonic membrane induced interactions between BAR domains, whose range is set by a characteristic lengthscale that depends on the bilayer moduli. In particular, the presence of a potentially significant energy barrier suggests that under certain conditions the BAR-domains may prefer to form an ordered array with a spacing of order ~10 nm, rather than a closely clustered domain.

Acknowledgments

Thanks to Dr D. Danino for her invaluable insights and help.

Conflicts of Interest

The author declares no conflicts of interest in this paper.

References

1. McMahon HT, Gallop JL (2005) Membrane curvature and mechanisms of dynamic cell membrane remodelling. *Nature* 438: 590–596.
2. Jao CC, Hegde BG, Gallop JL, et al. (2010) Roles of Amphipathic Helices and the Bin/Amphiphysin/Rvs (BAR) Domain of Endophilin in Membrane Curvature Generation. *J Biol Chem* 285: 20164–20170.
3. Mim C, Cui H, Gawronski-Salerno JA, et al. (2012) Structural basis of membrane bending by the N-BAR protein endophilin. *Cell* 149: 137–145.
4. Mim C, Unger VM (2012) Membrane curvature and its generation by BAR proteins. *Trends Biochem Sci* 37: 526–533.
5. Suarez A, Ueno T, Huebner R, et al. (2014) Bin/Amphiphysin/Rvs (BAR) family members bend membranes in cells. *Sci Rep* 4: 4693.
6. Liu S, Xiong X, Zhao X, et al. (2015) F-BAR family proteins, emerging regulators for cell membrane dynamic changes-from structure to human diseases. *J Hem & Onc* 8: 47.
7. Peter BJ, Kent HM, Mills IG, et al. (2004) BAR domains as sensors of membrane curvature: The amphiphysin BAR structure. *Science* 303: 495–499.
8. Blood PD, Voth GA (2006) Direct observation of Bin/amphiphysin/Rvs (BAR) domain-induced

membrane curvature by means of molecular dynamics simulations. *PNAS* 103: 15068–15072.
9. Blood PD, Swenson RD, Voth GA (2008) Factors influencing local membrane curvature induction by N-BAR domains as revealed by molecular dynamics simulations. *Biophys J* 95: 1866–1876.
10. Cui H, Ayton GS, Voth GA (2009) Membrane Binding by the Endophilin N-BAR Domain. *Biophys J* 97: 2746–2753.
11. Takei K, Slepnev VI, Haucke V, et al. (1999) Functional partnership between amphiphysin and dynamin in clathrin-mediated endocytosis. *Nature Cell Biol* 1: 33–39.
12. Frost A, Perera R, Roux A, et al. (2008) Structural basis of membrane invagination by F-BAR domains. *Cell* 132: 807–817.
13. Simunovic M, Mim C, Marlovits TC, et al. (2013) Protein-mediated transformation of lipid vesicles into tubular networks. *Biophys J* 105: 711–719.
14. Simunovic M, Srivastava A, Voth GA (2013) Linear aggregation of proteins on the membrane as a prelude to membrane remodeling. *PNAS* 110: 20396–20401.
15. Schweitzer Y, Kozlov MM (2015) Membrane-Mediated Interaction between Strongly Anisotropic Protein Scaffolds. *Plos Comput Biol* 11: e1004054.
16. Schweitzer Y, Shemesh T, Kozlov MM (2015) A model for shaping membrane sheets by protein scaffolds. *Biophys J* 109: 564–573.
17. Zimmerberg J, Kozlov MM (2006) How proteins produce cellular membrane curvature. *Nature Rev Molec Cell Biol* 7: 9–19.
18. Khelashvili G, Harries D, Weinstein H (2009) Modeling membrane deformations and lipid demixing upon protein-membrane interaction: The BAR dimer adsorption. *Biophys J* 97: 1626–1635.
19. Campelo F, Fabrikant G, McMahon HT, et al. (2010) Modeling membrane shaping by proteins: Focus on EHD2 and N-BAR domains. *Febs Lett* 584: 1830–1839.
20. Campelo F, Kozlov MM (2014) Sensing membrane stresses by protein insertions. *Plos Comput Biol* 10: e1003556.
21. Walani N, Torres J, Agrawal A (2014) Anisotropic spontaneous curvatures in lipid membranes. *Phys Rev E* 89: 062715.
22. Israelachvili JN (2011) Intermolecular and Surface Forces: Revised Third Edition: Elsevier Science.
23. Rawicz W, Olbrich KC, McIntosh T, et al. (2000) Effect of chain length and unsaturation on elasticity of lipid bilayers. *Biophys J* 79: 328–339.
24. Petrache HI, Tristram-Nagle S, Gawrisch K, et al. (2004) Structure and fluctuations of charged phosphatidylserine bilayers in the absence of salt. *Biophys J* 86: 1574–1586.
25. Tristram-Nagle S, Petrache HI, Nagle JF (1998) Structure and interactions of fully hydrated dioleoylphosphatidylcholine bilayers. *Biophys J* 75: 917–925.
26. Simunovic M, Voth GA (2015) Membrane tension controls the assembly of curvature-generating proteins. *Nature Commun* 6.
27. Simunovic M, Voth GA, Callan-Jones A, et al. (2015) When physics takes over: BAR proteins and membrane curvature. *Trends Cell Biol* 25: 780–792.
28. Dan N (2007) Lipid tail chain asymmetry and the strength of membrane-induced interactions between membrane proteins. *BBA- Biomembranes* 1768: 2393–2399.
29. Dan N (2007) Effect of lipid architecture on the properties of self-assembled membranes, and the

implications to protein-protein interactions. *Biophys J*: 548A–548A.
30. Helfrich W (1973) Elastic properties of lipid bilayers: theory and possible experiments. *Z Naturforsch C* 28: 693–703.
31. Kozlov MM, Leikin S, Rand RP (1994) Bending, hydration and interstitial energies quantitatively account for the hexagonal-lamellar-hexagonal reentrant phase-transition in dioleoylphosphatidylethanolamine *Biophys J* 67: 1603–1611.
32. Leikin S, Kozlov MM, Fuller NL, et al. (1996) Measured effects of diacylglycerol on structural and elastic properties of phospholipid membranes. *Biophys J* 71: 2623–2632.
33. Lipowsky R, Sackmann E (1995) Structure and dynamics of membranes: I. from cells to vesicles / II. generic and specific interactions: Elsevier Science.
34. ArandaEspinoza H, Berman A, Dan N, et al. (1996) Interaction between inclusions embedded in membranes. *Biophys J* 71: 648–656.
35. Masuda M, Mochizuki N (2010) Structural characteristics of BAR domain superfamily to sculpt the membrane, Elsevier, 391–398.
36. White SH, King GI (1985) Molecular packing and area compressibility of lipid bilayers. *PNAS* 82: 6532–6536.
37. Brannigan G, Brown FLH (2006) A consistent model for thermal fluctuations and protein-induced deformations in lipid bilayers. *Biophys J* 90: 1501–1520.
38. Zhou Y, Raphael RM (2007) Solution pH alters mechanical and electrical properties of phosphatidylcholine membranes: relation between interfacial electrostatics, intramembrane potential, and bending elasticity. *Biophys J* 92: 2451–2462.
39. Sapia P, Coppola L, Ranieri G, et al. (1994) Effects of high electrolyte concentration on DPPC-multilayers-An ESR and DSC investigation. *Colloid Poly Sci* 272: 1289–1294.
40. Risselada HJ, Marrink SJ (2009) Curvature effects on lipid packing and dynamics in liposomes revealed by coarse grained molecular dynamics simulations. *Phys Chem Chem Phys* 11: 2056–2067.
41. Nagle JF, Jablin MS, Tristram-Nagle S, et al. (2015) What are the true values of the bending modulus of simple lipid bilayers? *Chem Phys Lipids* 185: 3–10.
42. Arkhipov A, Yin Y, Schulten K (2009) Membrane-bending mechanism of Amphiphysin N-BAR domains. *Biophys J* 97: 2727–2735.
43. Bhatia VK, Hatzakis NS, Stamou D (2010) A unifying mechanism accounts for sensing of membrane curvature by BAR domains, amphipathic helices and membrane-anchored proteins. *Semin Cell Dev Biol* 21: 381–390.
44. Lyman E, Cui HS, Voth GA (2010) Water under the BAR. *Biophys J* 99: 1783–1790.
45. Ashkar R, Nagao M, Butler Paul D, et al. (2015) Tuning membrane thickness fluctuations in model lipid bilayers. *Biophys J* 109: 106–112.

AIMS Press